J Biomol NMR (2007) 37:79–95
DOI 10.1007/s10858-006-9105-y

ARTICLE

Observation of μs time-scale protein dynamics in the presence of Ln^{3+} ions: application to the N-terminal domain of cardiac troponin C

Christian Eichmüller · Nikolai R. Skrynnikov

Received: 20 September 2006 / Accepted: 2 October 2006 / Published online: 19 December 2006

Abstract The microsecond time-scale motions in the N-terminal domain of cardiac troponin C (NcTnC) loaded with lanthanide ions have been investigated by means of a $^1H^N$ off-resonance spin-lock experiment. The observed relaxation dispersion effects strongly increase along the series of NcTnC samples containing La^{3+}, Ce^{3+}, and Pr^{3+} ions. This rise in dispersion effects is due to modulation of long-range pseudocontact shifts by μs time-scale dynamics. Specifically, the motion in the coordination sphere of the lanthanide ion (i.e. in the NcTnC EF-hand motif) causes modulation of the paramagnetic susceptibility tensor which, in turn, causes modulation of pseudocontact shifts. It is also probable that opening/closing dynamics, previously identified in Ca^{2+}–NcTnC, contributes to some of the observed dispersions. On the other hand, it is unlikely that monomer–dimer exchange in the solution of NcTnC is directly responsible for the dispersion effects. Finally, on–off exchange of the lanthanide ion does not seem to play any significant role. The amplification of dispersion effects by Ln^{3+} ions is a potentially useful tool for studies of μs–ms motions in proteins. This approach makes it possible to observe the dispersions even when the local environment of the reporting spin does not change. This happens, for example, when the motion involves a 'rigid' structural unit such as individual α-helix. Even more significantly, the dispersions based on pseudocontact shifts offer better chances for structural characterization of the dynamic species. This method can be generalized for a large class of applications via the use of specially designed lanthanide-binding tags.

Keywords Cardiac troponin C · Spin-lock relaxation dispersion experiment · μs–ms protein dynamics · Lanthanide · Pseudocontact shift · Calmodulin

Electronic supplementary material Supplementary material is available in the online version of this article at http://www.dx.doi.org/10.1007/s10858-006-9105-y and is accessible for authorized users.

C. Eichmüller · N. R. Skrynnikov (✉)
Department of Chemistry, Purdue University, 560 Oval Drive, West Lafayette, IN 47907-2084, USA
e-mail: nikolai@purdue.edu

Present Address:
C. Eichmüller
Sandoz GmbH, Biochemiestraße 10, A-6250 Kundl, Austria

Introduction

Protein folding, protein–protein and protein–ligand interactions are all essentially dynamic processes that are often predicated on complex internal motions which occur on a μs–ms time scale. For studies of μs–ms dynamics a number of NMR experiments have been developed over the course of years (Palmer 2004; McDermott 2004). Notably, these experiments are uniquely suited for characterization of dynamic equilibria involving 'excited states', i.e. transient low-population species that often play a crucial role in the biological function of proteins (Mulder et al. 2001).

The data from NMR experiments are usually consistent with a simple two-state exchange model, where each of the states is characterized by distinct chemical shifts. The chemical shift difference between the two states, $\Delta\omega$, is central to NMR analyses of exchanging systems. Under fast exchange conditions, $\Delta\omega$ manifests itself through line broadening and can be accessed by means of relaxation dispersion experiments (Bloom

et al. 1965; Deverell et al. 1970). In this work we study the dynamic system where the difference in *chemical* shifts is augmented by the difference in *pseudocontact* shifts, induced by Ln^{3+} ions.

The proposed method is demonstrated for the N-terminal domain of cardiac troponin C. Troponin C (TnC) is a dumbbell-shaped protein which, together with troponin I (TnI) and T (TnT), forms the troponin assembly. The C-terminal lobe of TnC possesses two high-affinity metal-binding sites that are permanently occupied under physiological conditions. This domain plays a structural role as it anchors the N-terminal helix of TnI. In contrast, the N-terminal domain (NcTnC) serves as a Ca^{2+}-regulated molecular switch. Only one of the two EF-hand motifs in NcTnC is capable of binding calcium—the other site is defunct due to alteration of the two ligand residues. Upon loading a single Ca^{2+} ion, NcTnC switches to the dynamic state that is primed for binding (Pääkkönen et al. 1998; McKay et al. 2000; Eichmüller and Skrynnikov 2005) and, consequently, locks onto a short amphiphilic helix III from TnI (Li et al. 1999). As a result, a large portion of TnI is displaced, including the two so-called inhibitory regions located up- and down-stream from the helix III (Farah et al. 1994; Takeda et al. 1997; Luo et al. 2000). These inhibitory regions are lifted off of their binding sites on the surface of actin, thereby bringing about changes in the actin-tropomyosin assembly and clearing the way for actin–myosin binding. The result is a contraction of a striated muscle (Kobayashi and Solaro 2005).

Like other calcium-binding proteins (Campbell et al. 1975; Lee and Sykes 1983; Bentrop et al. 1997), NcTnC binds Ln^{3+} ions in its calcium-binding site (Wang et al. 1981; Gay et al. 2004). Lanthanide ions have a well-established record as useful structural probes in NMR (Lee and Sykes 1983; Dwek et al. 1971), X-ray crystallography (Weis et al. 1991; Burling et al. 1996), and luminescence spectroscopy of proteins (Rhee et al. 1981). Particularly, in NMR studies contact and pseudocontact shifts, various relaxation enhancement parameters, and residual dipolar couplings due to Ln^{3+}-induced alignment were all used for protein structure determination (Bertini et al. 2001a). In addition, Ln^{3+}-for-Ca^{2+} substitution helps to elucidate the structural mechanism of calcium regulation (Mustafi et al. 2004; Dudev et al. 2005). In this work we extend the scope of Ln^{3+} applications by demonstrating that lanthanides can be used to 'highlight' the effects of μs–ms time-scale motion in proteins.

We have prepared the samples NcTnC with La^{3+}, Ce^{3+}, and Pr^{3+} ions and used our recent proton off-resonance spin lock experiment (Eichmüller and Skrynnikov 2005) to record relaxation dispersion profiles. In the presence of paramagnetic lanthanides the dispersion amplitudes were strongly increased. We attribute this effect primarily to μs time-scale dynamics in the lanthanide binding site. This dynamics leads to *modulation of paramagnetic susceptibility tensor* which, in turn, causes modulation of long-range pseudocontact shifts and thus gives rise to line broadening and dispersion effects.

We have also analyzed other possible forms of dynamics contributing to Ln^{3+}-induced dispersions. The data suggest that *opening/closing* motion such as identified in Ca^{2+}-NcTnC may well contribute to the observed dispersions. On the other hand, it is unlikely that *transient dimerization* of Ln^{3+}-NcTnC is directly responsible for the dispersion effects, although it may influence other forms of μs motion. *On-off exchange* of Ln^{3+} ion does not seem to be a significant factor under the conditions of our experiments, and there is no reason to suggest a presence of secondary Ln^{3+}-binding sites.

In conclusion, we discuss the prospects for using Ln^{3+} ions as probes of native protein dynamics in the μs–ms range. Remarkably, long-range pseudocontact shifts can generate large dispersions where chemical shifts fail because of their local nature. Even more significantly, the values of $\Delta\omega$ associated with pseudocontact shifts can be readily converted into structural parameters. This paves the way for the structural characterization of the exchanging species, which is especially valuable in the case of the elusive 'excited states'. However, this approach is feasible only if the Ln^{3+} ion is tightly bound in a well-defined static environment and does not interfere with native protein dynamics. From this perspective, lanthanide-binding tags present an attractive and sufficiently general option.

Observation and analysis of Ln^{3+}-induced dispersions

The affinity of Ca^{2+} to NcTnC is ca. 3 μM at 30°C (Li et al. 1997; Hazard et al. 1998) and probably somewhat tighter at lower temperatures (Li et al. 2002). The titration of Ca^{2+}, therefore, proceeds under intermediate-to-fast exchange conditions with each resonance moving in a continuous fashion. In contrast, the La^{3+}, Ce^{3+} and Pr^{3+} titration is characterized by a slow exchange regime, with apo and holo forms giving rise to distinct sets of peaks. In this situation, one cannot rely on a lanthanide titration to obtain complete spectral assignment of Ln^{3+}-NcTnC. Instead, a set of triple-resonance experiments was executed for each of the three samples and the backbone assignment was thus obtained. The ^{1}H,^{15}N-HSQC spectra of the

NcTnC samples loaded with different ions are presented in Fig. 1.

The analysis of the lineshapes in the course of the lanthanide titrations established that the Ce^{3+} off-rates at 30°C are in the range of 15–25 s^{-1}, while Pr^{3+} off-rates at 10°C are 5–10 s^{-1}. Assuming that lanthanides bind to NcTnC in diffusion-controlled manner, just like calcium (Hazard et al. 1998; Li et al. 2002), one obtains $K_D \approx 0.1\mu M$, in agreement with previous results (Wang et al. 1981). This binding is sufficiently tight to avoid unwanted complications from on-off exchange (discussed in more detail later).[1]

The spectra shown in Fig. 1 were used to determine pseudocontact shifts according to $\delta_{pc}(Ln^{3+}) = \delta(Ln^{3+}) - \delta(La^{3+})$, where Ln^{3+} is a paramagnetic ion (Ce^{3+} or Pr^{3+}) and La^{3+} is diamagnetic lanthanum ion used as a reference.[2] The resulting δ_{pc} data were fitted to the well-known expression:

$$\delta^i_{pc} = \frac{\Delta\chi_a}{12\pi r_i^3}\left\{(3\cos^2\theta_i - 1) + \frac{3}{2}R\sin^2\theta_i\cos 2\phi_i\right\} \quad (1)$$

where $\Delta\chi_a$ is the axial component of the (traceless) magnetic susceptibility tensor of the Ln^{3+} ion in its binding site, R is the rhombicity of this tensor, θ_i and ϕ_i describe the orientation of the vector connecting the Ln^{3+} ion with the spin of interest relative to the principal axes of the susceptibility tensor, and r_i is the corresponding distance (Bertini et al. 2001c). The total of 117 and 98 experimentally measured pseudocontact shifts (Ce^{3+} and Pr^{3+} data sets, respectively) have been fitted with Eq. 1 using the NMR structure of Ca^{2+}-NcTnC 1AP4 (Spyracopoulos et al. 1997). The results of the fitting, Fig. 2, can be taken as a confirmation that the Ln^{3+}-for-Ca^{2+} substitution does not cause any major structural perturbations in the protein.

The degree of correlation observed in Fig. 2, $r = 0.89$, is somewhat lower than what is typically obtained for Ln^{3+}-loaded proteins (Banci et al. 1996; Baig et al. 2004). For instance, for Dy^{3+}-doped α-parvalbumin the correlation coefficient $r = 0.95$ has been obtained based on a similar fitting procedure (Baig et al. 2004). One should bear in mind, however, that (*i*) Dy^{3+} generates much larger shifts than Ce^{3+} or Pr^{3+}, (*ii*) in contrast to NcTnC, parvalbumin has very little internal motion (Baldellon et al. 1998), and, on a related note, (*iii*) the structural model of parvalbumin has somewhat higher precision. Of note, Ca^{2+}-NcTnC also produced a relatively poor fit in the study employing ^{15}N-^{1}H residual dipolar couplings (r around 0.8 for a number of structural models, including 1AP4) (Pääkkönen et al. 2000).

The sizeable pseudocontact shifts, up to 0.6 ppm, observed in Ce^{3+}- and Pr^{3+}-NcTnC spectra (Fig. 2) offer new possibilities for studies of μs–ms time scale dynamics in this protein. Toward this goal, we recorded a large set of relaxation dispersion data in the Ln^{3+}-loaded samples of NcTnC. The details of the experiment, developed with Ln^{3+}-loaded proteins in mind, were recently reported (Eichmüller and Skrynnikov 2005). In designing this experiment we recognized that pseudocontact shifts, as expressed in ppm, do not depend on the spin's Larmor frequency. Therefore, in the case of chemical exchange the frequency modulation associated with pseudocontact shifts, $\Delta\omega = \omega_0\Delta\delta_{pc}$, is much larger for protons than for heteronuclei. Thus, proton is the nucleus of choice for detecting Ln^{3+}-induced dispersions (conversely, if the goal is to observe Ln^{3+}-induced dispersions on heteronuclei, then conventional HSQC-based schemes should be abandoned because of the severe broadening in the proton dimension and direct-detection schemes (Machonkin et al. 2002) should be employed instead).

The main difficulty in the proton relaxation dispersion experiments stems from extensive cross-relaxation and scalar coupling between numerous proton spins. To minimize these effects we implemented a number of solutions: (i) used deuterated samples with protons exchanged into amide positions (Ishima et al. 1998), (ii) employed off-resonance spin lock with the constant tilt angle of 35° (Desvaux et al. 1995), and (iii) utilized the spin mode with anti-phase character with respect to nitrogen, $(H_x + 2H_z)N_z$. Large effective *rf* fields obtainable in this experiment allow one to target faster forms of motion, down to several microseconds. Figure 3 shows the representative relaxation dispersion curves obtained from our constant-angle off-resonance $^{1}H^{N}$ spin lock experiment conducted on four holo-NcTnC samples. The relaxation rates determined in this experiment are, in a very good approximation, given by (Eichmüller and Skrynnikov 2005):

$$\bar{R}^{mod}_{1\rho} = R_{ex} + (R_{anti} - R_{zz}) \quad (2)$$

where R_{anti} and R_{zz} are the relaxation rates of H_xN_z and H_zN_z, respectively. The exchange contribution R_{ex}

[1] La^{3+}, Ce^{3+}, and Pr^{3+} have similar effective ionic radii, 1.10–1.06 Å, and therefore are all expected to bind in a similar fashion. Smaller ions, on the other hand, can behave differently. Indeed, we found that Yb^{3+} (0.92 Å) binds to NcTnC in the intermediate-to-fast exchange regime.

[2] Note that paramagnetic lanthanide ions also produce weak alignment (Contreras et al. 1999; Biekofsky et al. 1999) so that the experimentally measured differences $\delta(Ln^{3+}) - \delta(La^{3+})$ contain, generally speaking, a residual CSA component (John et al. 2005). It is easy to estimate, however, that with the present very small degree of alignment the residual CSA shifts do not exceed 0.01 ppm and therefore can be safely ignored.

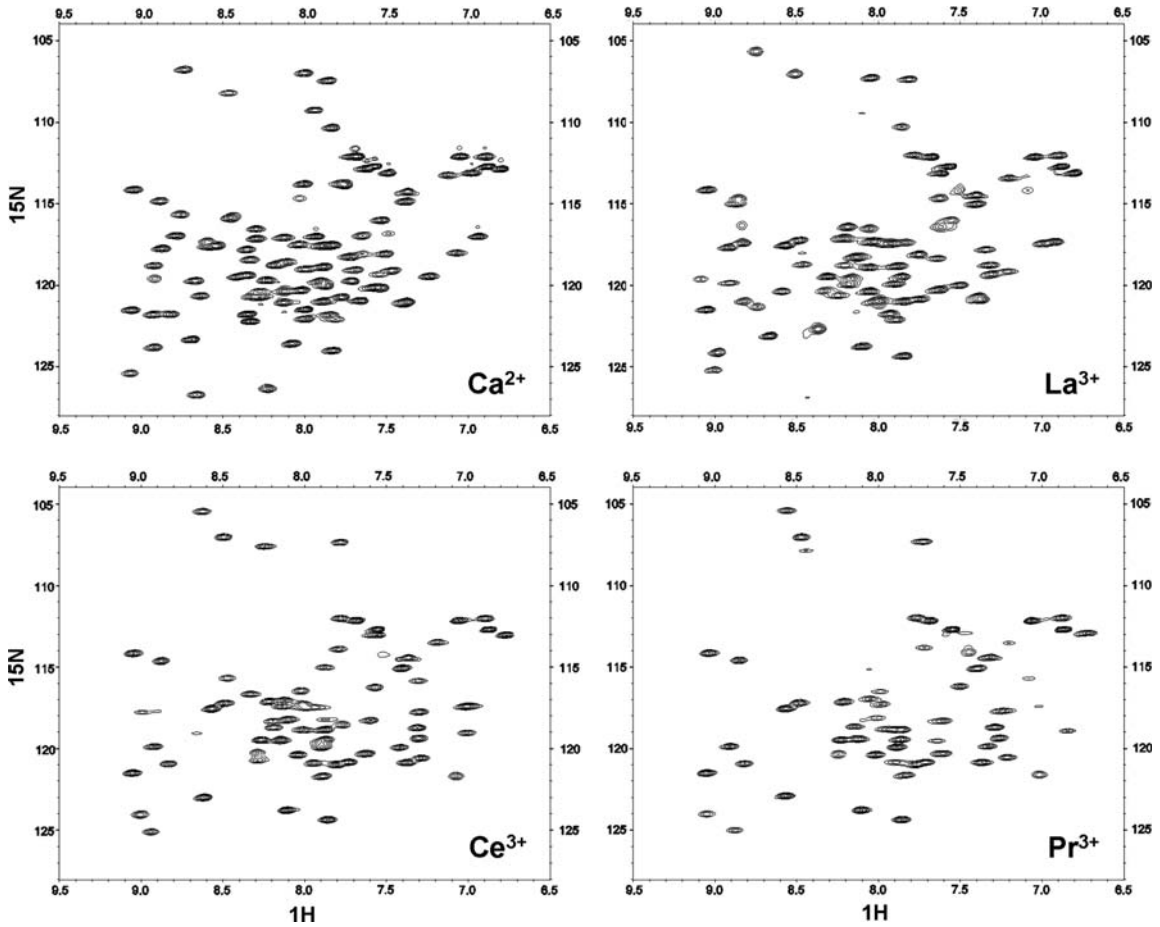

Fig. 1 $^{1}H,^{15}N$ HSQC spectra of Ca^{2+}-, La^{3+}-, Ce^{3+}-, and Pr^{3+}-NcTnC at 10°C, 600 MHz. The samples contained 1.2, 1.2, 2.0, and 2.0 mM of protein, respectively. The measurement times were adjusted to compensate for the difference in concentration; the spectra were plotted at the same contour level. Metal ion content was 4.0, 1.25, 1.25, and 1.25 molar equivalents, respectively. In the case of Ca^{2+}, the peaks from Gly 70 and Val 72 are outside the plotted spectral region. The tables of spectral frequencies for Ln^{3+}-NcTnC (C35S, C84S) are given in the Supplementary Materials

for the system in question falls in the Redfield limit; in a two-state approximation, this term is expressed as (Deverell et al. 1970):

$$R_{ex} = p_a p_b (\omega_0 \Delta\delta)^2 \frac{\tau_{ex}}{1 + (\omega_1^{eff} \tau_{ex})^2} \quad (3)$$

The dependence of the recorded dispersion profiles on the static magnetic field confirms that the observed exchange is fast (see Fig. 3) (Millet et al. 2000).

The curves presented in Fig. 3 illustrate two types of behavior. Residue 14 shows no dispersion in any of the samples. Apparently, there is no local motion that could modulate the $^{1}H^{N}$ chemical shift in this residue. This residue is also located too far from the metal center (Ce^{3+}, Pr^{3+}) to sense any significant pseudocontact shift. The situation is different in residue 42. This residue shows no discernible dispersion in the diamagnetic Ca^{2+}-NcTnC and La^{3+}-NcTnC samples. The dispersion appears, however, in the sample containing a weak paramagnetic ion, Ce^{3+}-NcTnC. It is amplified in the presence of the stronger paramagnetic ion, Pr^{3+}-NcTnC. This kind of behavior unequivocally suggests that the observed dispersions are caused by modulation of the pseudocontact shifts.

A systematic comparison of the dispersion profiles, beyond the two examples shown in Fig. 3, reveals a more complex pattern. Nonetheless, the general trend is unmistakable: paramagnetic Ln^{3+} ions tend to magnify the dispersion effects in this protein. This is demonstrated in Fig. 4 where the fitted values of $p_a p_b (\Delta\delta)^2$ obtained from the analyses of the relaxation dispersion data are plotted as a function of residue number (the corresponding τ_{ex} values are presented in Fig. 5).

First, compare the results from the two diamagnetic samples, Ca^{2+}-NcTnC and La^{3+}-NcTnC (two top panels in Fig. 4). It is immediately obvious that there are substantial differences in the dynamic behavior of

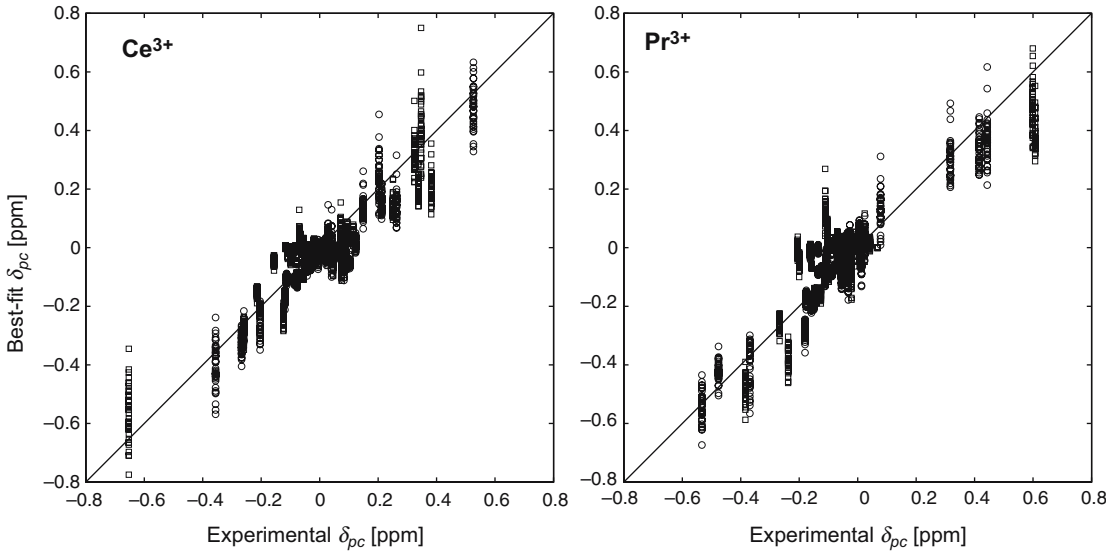

Fig. 2 The correlation between experimental and fitted pseudocontact shifts in Ce^{3+}- and Pr^{3+}-NcTnC. The experimental data are from ^{1}H,^{15}N-HSQC spectra recorded at 10°C at 600 MHz. Pseudocontact shifts of $^{1}H^{N}$ (circles) and ^{15}N (squares) have been included in the fitting procedure with the same weight. Protein coordinates used in the fitting are from the PDB structure 1AP4 (Spyracopoulos et al. 1997), where Ca^{2+} has been replaced with Ln^{3+}. A single susceptibility tensor has been determined in the course of the fitting procedure using all 40 conformations from 1AP4 as structural input (Banci et al. 1996; Eichmüller and Skrynnikov 2005). The best-fit parameters are $\Delta\chi_a = 1.01 \cdot 10^{-26}$ ppm m^3, $R = 0.54$, $\alpha = 33°$, $\beta = 120°$, $\gamma = 6°$ for Ce^{3+}-NcTnC and $\Delta\chi_a = 1.65 \cdot 10^{-26}$ ppm m^3, $R = 0.57$, $\alpha = 31°$, $\beta = 126°$, $\gamma = 2°$ for Pr^{3+}-NcTnC. The Euler angles α, β, γ specify the orientation of the susceptibility tensor principal axes in the molecular frame 1AP4. The correlations presented in the plot are characterized by $r = 0.89$, $Q = 0.47$ and $r = 0.89$, $Q = 0.46$ for the left and right panels, respectively. In addition to 1AP4 we have also tested other sets of coordinates: NMR structure 1MXL (Li et al. 1999) (entire ensemble as well as individual conformations) and crystallographic structure 1J1D (Takeda et al. 2003). Furthermore, the fitting procedure was repeated using the reduced δ^{i}_{pc} data set where we excluded the data from terminal helix D (likely to be affected by protein dimerization, see below). None of these modifications caused any significant change in the quality of data fitting or in the extracted susceptibility parameters

the two samples. The important feature of La^{3+}-NcTnC is the mobility of the metal-binding EF-hand. Within the twelve-residue calcium-binding segment, the resonances from residues 70 and 72 are unobservable, the resonances from residues 66, 67, 69, and 73 are unobservable at 10°C but appear as weak and broadened peaks at 30°C, and residues 65, 68, 71, 75, and 76 show pronounced dispersion effects. The list of the affected residues includes all five of the canonical EF-hand ligands. This is in sharp contrast to Ca^{2+}-NcTnC, where all twelve resonances are present and none of them shows statistically significant dispersion effects.

While at first this contrasting behavior seems surprising, it can be rationalized. NcTnC is a molecular switch with a finely tuned response to calcium binding (McKay et al. 2000). Although a good mimetic of calcium, La^{3+} carries an extra charge which is likely to perturb the delicate equilibrium existing in the Ca^{2+}-loaded NcTnC. The result is 'dynamization' of the metal-binding site, residues 65–76. The changes are transmitted to the other parts of the protein via the network of hydrogen bonds, and the defunct calcium-binding site, residues 29–40, apparently responds to that by becoming more rigid. Of course, the disappearance of dispersions in this situation may also mean a shift in the time scale of motion which would render it unobservable for spin-lock measurements.

We shall turn now to the comparison of lanthanide-loaded samples (three lower panels in Fig. 4). In the vicinity of the metal-binding site, residues 50–80, the comparison is hardly possible since most resonances in the Ce^{3+} and Pr^{3+} samples are broadened beyond detection. The major source of this broadening is a Curie spin relaxation (Guéron 1975; Vega and Fiat 1976) and hence no assumptions can be made about the effects of exchange. However, the remaining portion of the protein, residues 3–50, lends itself to comparison. The data in Fig. 4 clearly show that the amplitude of dispersion effects increases in going from diamagnetic La^{3+} to weakly paramagnetic Ce^{3+} and then to moderately paramagnetic Pr^{3+}. This demonstrates, on a sufficiently large set of data, that modulation of pseudocontact shifts by exchange can be an effective mechanism of line broadening.

The important question that remains is: what type of molecular motion is responsible for modulation of

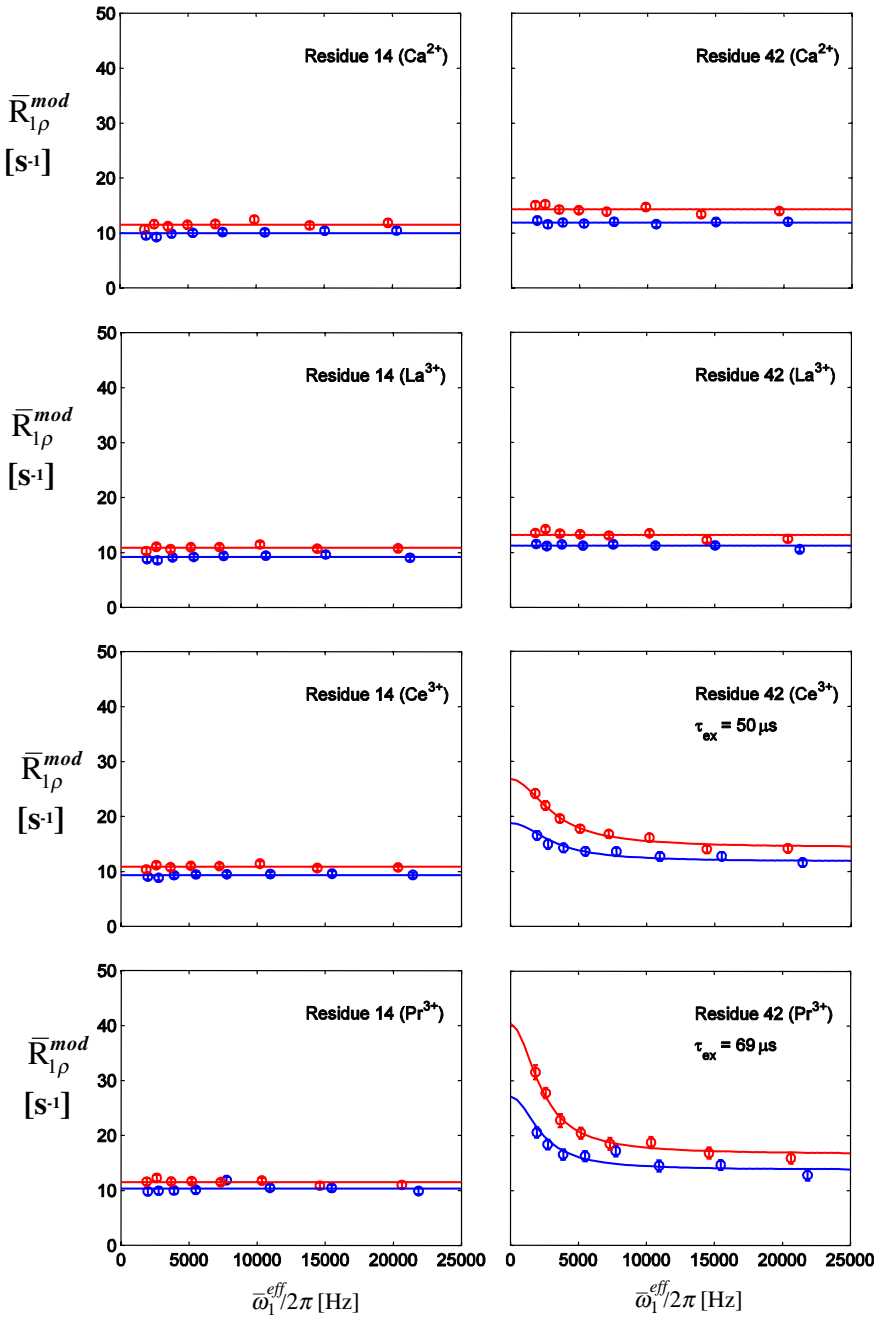

Fig. 3 Representative relaxation dispersion profiles obtained from Ca^{2+}-, La^{3+}-, Ce^{3+}-, and Pr^{3+}-NcTnC using constant-angle off-resonance proton spin-lock experiment. The data have been collected at 600 and 800 MHz (blue and red circles, respectively). The exchange correlation times indicated for Ce^{3+}- and Pr^{3+}-NcTnC have the error intervals 39–62 and 53–91 μs, respectively. The details of the experiment, the fitting procedure, and the Ca^{2+}-NcTnC results have been reported previously (Eichmüller and Skrynnikov 2005). The presented curves illustrate typical quality of the data. For example, if all data are ranked according to the fit residual, residue 42 consistently ranks in the 45–55 percentile

pseudocontact shifts? This question is addressed in the next section.

Possible dynamic scenarios for Ln^{3+}-induced dispersions

Modulation of χ by internal motion in the Ln^{3+}-binding site

We suggest that the primary cause of Ln^{3+}-induced dispersions observed in NcTnC is the modulation of the susceptibility tensor χ by μs time-scale motion which occurs in the lanthanide-binding site. The modulation of χ automatically leads to modulation of pseudocontact shifts, cf. Eq. 1, which in turn leads to extensive dispersion effects. What is the evidence for this scenario? First of all, μs time-scale dynamics in lanthanide-loaded EF hand is directly observed in the diamagnetic La^{3+}-NcTnC sample (second panel in Fig. 4). As discussed above, the motion involves all lanthanide ligands. Note that even a slight rearrangement of the low-symmetry Ln^{3+} environment could be sufficient to alter the orientation of the χ principal axes

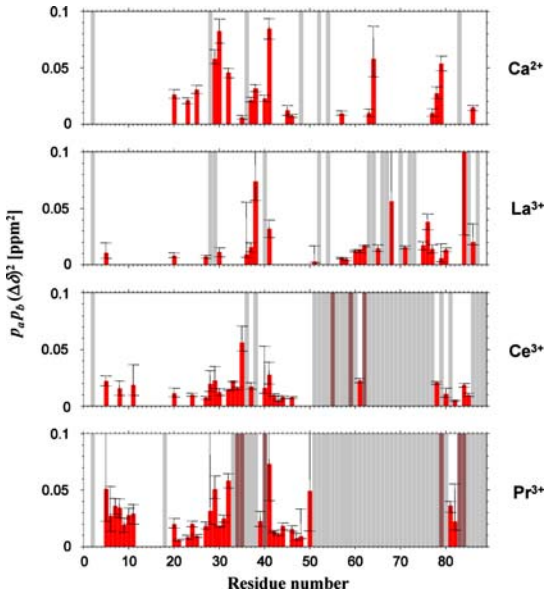

Fig. 4 Best-fit values of $p_a p_b(\Delta\delta)^2$ obtained from fitting of $^1H^N$ relaxation dispersion data in Ca^{2+}-, La^{3+}-, Ce^{3+}-, and Pr^{3+}-NcTnC. Empty slots in the histogram indicate the absence of dispersion. Red bars represent $p_a p_b(\Delta\delta)^2$ values. Grey bars indicate missing data (this includes Pro 52 and Pro 54, a number of resonances that have been assigned at 30°C but disappear from the spectrum at 10°C, and several heavily overlapped peaks). Pink bars correspond to severely broadened peaks where dispersion is identifiable by eye, but is not picked up by the model selection criterion (Eichmüller and Skrynnikov 2005) because of the poor signal-to-noise ratio

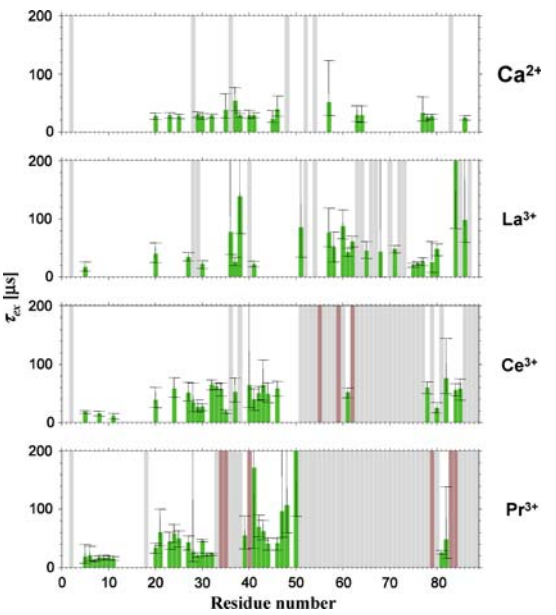

Fig. 5 Best-fit values of τ_{ex} obtained from fitting of $^1H^N$ relaxation dispersion data in Ca^{2+}-, La^{3+}-, Ce^{3+}-, and Pr^{3+}-NcTnC. The conventions are the same as in Fig. 4

and thereby cause effective modulation of the shifts. In this situation it is almost certain that χ undergoes efficient μs time-scale modulation.

Let us assume for a moment that the μs time-scale motion in the binding site can be viewed as a two-state exchange. The observed pseudocontact shifts in this case will be given by $p_a\delta^a_{pc} + p_b\delta^b_{pc}$, while the corresponding dispersion parameters will be $p_a p_b(\delta^a_{pc} - \delta^b_{pc})^2$. Although there is no reason to expect a strong correlation between these two quantities, a certain pattern should exist—for instance, both quantities disappear for those $^1H^N$ spins that are far removed from the paramagnetic center. Indeed, out of 10 amide protons with the smallest pseudocontact shifts only 2 show dispersions, while among 10 protons with the largest shifts 9 show dispersions (Ce^{3+}-NcTnC data; the results for Pr^{3+}-NcTnC are similar). This is compatible with the proposed scenario whereby the dispersions are caused by modulation of χ.

In this context it is also worth noting that the values of $\Delta\chi_a$ determined in our analyses, Fig. 2, are two times lower than those found in another EF-hand protein, calbindin D_{9k} (Bertini et al. 2001b; Allegrozzi et al. 2002). In line with the evidence discussed above, this is suggestive of motional averaging of χ in Ln^{3+}-NcTnC.

Within the framework of the present scenario it is also possible to rationalize the τ_{ex} data, Fig. 5. In the lanthanide-loaded samples, τ_{ex} values show some variability (in particular, shorter τ_{ex} are observed near the N-terminus). If one assumes that the motion in the Ln^{3+}-binding site is actually more complex than two-state exchange, it is easy to see how different portions of the protein structure may sense somewhat different time scales.[3] This kind of τ_{ex} variability is common for more complex forms of exchange in proteins (Mulder et al. 2001). Of note, there is much less variability in simple situations such as on-off exchange (Millet et al. 2002).

While no high-resolution coordinates are available for Ln^{3+}-NcTnC, inspection of calcium-loaded structures 1AP4 and 1MXL (Li et al. 1999) offers a hint as to the possible origins of μs time-scale dynamics in the binding site. The coordination of calcium by carboxylate oxygens of Asp 65 and Asp 67 shows substantial variability. In particular, the side chain of Asp 67

[3] For the sake of example, suppose that the binding site in Ln^{3+}-NcTnC adopts three different conformations, giving rise to pseudocontact shifts δ^a_{pc}, δ^b_{pc}, and δ^c_{pc}. Further suppose that for a certain amide the orientation of the Ln^{3+}–$^1H^N$ vector is such that δ^a_{pc} and δ^b_{pc} are degenerate, whereas δ^c_{pc} takes a distinctive value. Under these circumstances, the dispersion profile will be sensitive to the exchange rates k_{ac} and k_{bc}, but essentially independent of k_{ab}. If the dispersion data are subsequently fitted with the two-state model (which usually produces a satisfactory fit) then the derived τ_{ex} will be representative of k_{ac} and k_{bc}, but not of k_{ab}. Reasoning along these lines, one can see how different $^1H^N$ sites may report somewhat different τ_{ex} values.

samples different conformations with regard to χ_1, which directly affects the ligation of Ca^{2+}. Furthermore, in the structure 1MXL the side chain of Asp 65 turns out to be poorly localized with respect to Ca^{2+}. Occasionally, both aspartate side chains form hydrogen bonds with the backbone amide groups. In summary, the analysis of NMR coordinates suggests that there is room for dynamics in the metal-binding site of NcTnC.

In this context it is interesting to point out that μs time-scale dynamics has been observed in the asparatic acid residue which ligates calcium in P43M mutant of calbindin D_{9k} (Bertini et al. 2002). Another well-characterized example of a dynamic binding site occurs in the Ca^{2+}-saturated E140Q mutant of the C-terminal domain of calmodulin (E140Q-CCaM). In this protein extensive motions have been observed not only in the binding site that is compromised by the mutation (129–140), but also in the intact site (93–104) (Evenäs et al. 1999). A molecular dynamics study suggests that replacement of one Ca^{2+} ligand by a water molecule may be implicated in this process (Likic et al. 2003). The motion has been characterized as a two-state equilibrium involving open and closed conformations. The populations of the two species are approximately equal and the time scale of the exchange is ca. 20 μs (Evenäs et al. 1999; Lundström and Akke 2004). One cannot help but notice the similarity with Ca^{2+}-NcTnC, where one of the calcium-binding sites is defunct, and the time scale of motion is 30 μs (Eichmüller and Skrynnikov 2005).

The possibility of conformational exchange has been also noted in the systems where Ln^{3+} is substituted for Ca^{2+}. While the usual coordination number of Ln^{3+} in the EF-hand motif is seven, octa-coordinated Yb^{3+} has been found in the second site of carp parvalbumin (Kumar et al. 1991). The difference is due to Asp 92 which ligates Yb^{3+} via both carboxylate oxygens (this residue is equivalent of Asp 67 in NcTnC). The metal-binding site also proved to be flexible as indicated by the elevated temperature factors. In another study, Pidcock and Moore showed, by analyzing selected protein structures, that Ln^{3+}-for-Ca^{2+} substitution tends to weaken the hydrogen bonding network around the metal-binding site (Pidcock and Moore 2001). While little information is available about proteins, in the case of small chelating complexes it is well known that bound ligands (including bidentate ligands) can rapidly interchange positions on the surface of the lanthanide ion and exchange with ligands that are not bound to the ion (Peters et al. 1996; Pidcock and Moore 2001; Parker et al. 2002). All this evidence supports the notion of dynamic lanthanide environment in Ln^{3+}-NcTnC.

Opening/closing dynamics

The most interesting possibility is that Ln^{3+}-NcTnC retains much of the internal dynamics that occurs in Ca^{2+}-NcTnC. If that is the case, then Ln^{3+}-induced dispersion should reflect this 'native' dynamics—notably, the opening/closing motion proposed for Ca^{2+}-NcTnC. This possibility is discussed below in detail.

Calmodulin-family proteins rely on a pair of sequential helix-loop-helix motifs to execute their function. In the apo protein, the two motifs are in UU-configuration, which corresponds to a closed form. In response to calcium binding, they switch to a more open L ⅃ conformation. The opening exposes a hydrophobic surface and thus allows proteins to bind their molecular targets.

NcTnC does not quite conform to the usual rules. Only one of the two EF-hands in NcTnC binds calcium, and the binding fails to achieve complete opening of the structure (Spyracopoulos et al. 1997). Instead, it is believed that Ca^{2+}-NcTnC establishes dynamic equilibrium between the closed and open forms, with the closed form prevailing (Pääkkönen et al. 1998; McKay et al. 2000; Gaponenko et al. 1999). The protein can be locked in the open form when presented with a suitable molecular target, such as troponin I (Li et al. 1999) or bepridil (Li et al. 2000). The transition from the closed to open structure involves reorientation of helices B and C which move as a single unit in the direction away from the metal-binding site. Previously, this type of opening/closing dynamics has been identified in $(Ca^{2+})_2$-E140Q-CCaM (Evenäs et al. 1999) and proposed for apo-CCaM (Malmendal et al. 1999; Tjandra et al. 1995).

The concept of dynamic equilibrium involving closed and open forms of Ca^{2+}-NcTnC is consistent with our relaxation dispersion data (Fig. 4, upper panel). This is illustrated in Fig. 6. The left part of the figure shows dynamic residues, as identified in our relaxation dispersion measurements (Eichmüller and Skrynnikov, 2005), mapped onto the structure of the protein. The right part shows the residues that undergo a large change in dihedral angles ϕ, ψ upon opening of the protein structure (Spyracopoulos et al. 1997; Li et al. 1999). The correspondence between the two plots suggests that relaxation dispersions in Ca^{2+}-NcTnC arise, to a large extent, from the opening/closing of the molecular structure. Another source of dispersions is the inherent flexibility of the defunct Ca^{2+}-binding site.

Given the presence of opening/closing dynamics in Ca^{2+}-NcTnC, it is possible that this type of motion is also responsible for Ln^{3+}-induced dispersion effects. To test this hypothesis, we simulated the expected

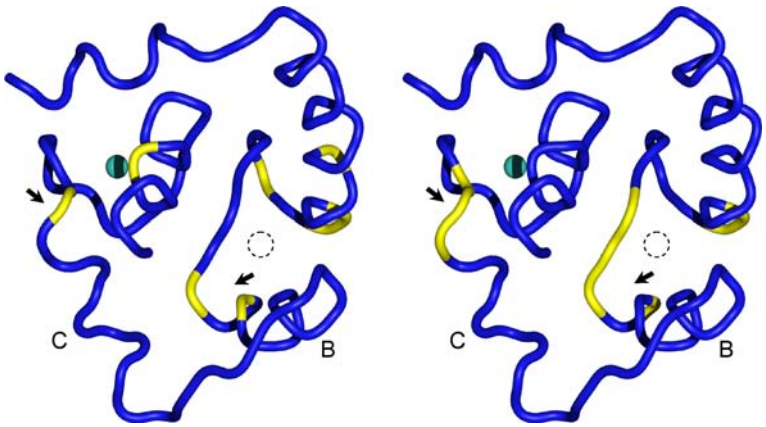

Fig. 6 Opening/closing in Ca^{2+}-NcTnC. Left part: color-coded yellow are the residues with substantial dispersion amplitude, $p_a p_b(\Delta\delta)^2 > 0.03$ ppm^2 (see upper panel in Fig. 4). Right part: color-coded yellow are the residues with $(\Delta\phi^2 + \Delta\psi^2)^{1/2} > 40°$, where $\Delta\phi$ and $\Delta\psi$ are the differences in the mean backbone dihedral angles between the closed structure 1AP4 and the open structure 1MXL. The wireframe representation is that of the mean structure 1AP4 (minus flexible termini). Cyan sphere is the Ca^{2+} ion, dashed circle marks the defunct binding site, the arrows indicate the residues that play the role of hinges in the opening/closing of Ca^{2+}-NcTnC, symbols B and C denote the corresponding helices

dispersion effects. We started by re-fitting the susceptibility tensor based on a reduced experimental data set. Excluded were all δ_{pc} data from helices B and C (residues 38–64). The retained portion of the protein, which includes the metal-binding site, is deemed static and insensitive to the conformational exchange (in doing so we ignore the internal motions discussed in the previous section). The fitted susceptibility tensor was used to predict δ_{pc} values in the closed structure 1AP4 and, separately, in the open structure 1MXL. The results were then subtracted to obtain $\Delta\delta_{pc}$ which describes the presumed modulation of pseudocontact shifts by conformational exchange. Finally, the quantity $p_a p_b(\Delta\delta_{pc})^2$ was evaluated, assuming that p_a is equal to 0.2 (McKay et al. 2000; Eichmüller and Skrynnikov 2005).

The simulated $p_a p_b(\Delta\delta_{pc})^2$ values plotted in Fig. 7 can be directly compared with the experimental results, two lower panels in Fig. 4. Such comparison shows that conformational exchange is likely to have a hand in Ln^{3+}-induced dispersions for part of the defunct calcium-binding site and helix B (i.e. the region extending from residue 33 to residue 45). For instance, this model could explain the emergence of dispersion effect in residue 42, as illustrated in Fig. 3. This residue is a part of helix B which moves as a rigid unit when NcTnC undergoes transition from the closed to open form. Because the local environment of the $^1H^N$ from residue 42 does not change with motion, it shows no exchange broadening and no dispersion in the Ca^{2+}- and La^{3+}-NcTnC samples. On the contrary, in the Ce^{3+}- and Pr^{3+}-NcTnC samples opening/closing leads to efficient modulation of δ_{pc} and hence gives rise to the dispersion effect.

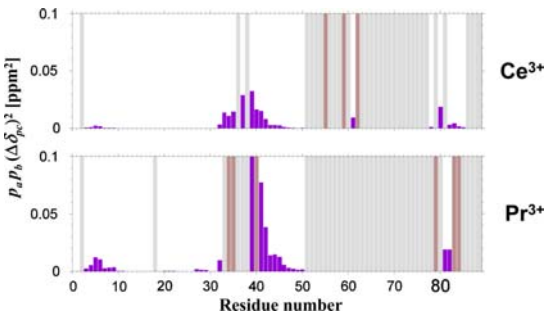

Fig. 7 Simulated $p_a p_b(\Delta\delta_{pc})^2$ values (purple bars) for the model of conformational exchange in Ce^{3+}- and Pr^{3+}-NcTnC. The format is the same as in Fig. 4. Open and closed forms of Ln^{3+}-NcTnC were modeled by the NMR coordinates 1MXL and 1AP4, respectively. Prior to calculations, two structures were transformed into the same coordinate frame by superimposing their calcium-binding sites. The susceptibility tensors were determined using the invariant portion of the structure (δ_{pc} data from residues 38–64 were excluded, as described in the text). The best-fit parameters are $\Delta\chi_a = 1.14 \cdot 10^{-26}$ ppm m^3, $R = 0.64$, $\alpha = 30°$, $\beta = 122°$, $\gamma = 1°$ for Ce^{3+}-NcTnC and $\Delta\chi_a = 2.59 \cdot 10^{-26}$ ppm m^3, $R = 0.64$, $\alpha = 35°$, $\beta = 123°$, $\gamma = 4°$ for Pr^{3+}-NcTnC. In the latter case, $\Delta\chi_a$ is likely overestimated because the truncated data set contains only a few pseudocontact shifts that are not small. The above susceptibility parameters have been used to predict the values of δ_{pc} in 1AP4 and 1MXL and further calculate the difference, $\Delta\delta_{pc} = \delta^a_{pc} - \delta^b_{pc}$

Although this model can account for some of the experimental findings, it generally fails to predict strong dispersions observed in helices N and A (residue 3 to 28). In this situation it is difficult to make any claims with regard to observation of the exchange between open and closed conformations of NcTnC. It is almost certain that the competing mechanism—modulation of susceptibility tensor by local dynamics in the

binding site—is operational. It would be difficult to separate the two effects.

At the same time, one can take a view that the opening/closing in Ca^{2+}-NcTnC and the fluxionality of the metal-binding site in Ln^{3+}-NcTnC are nothing else than different manifestations of the vast dynamic network existing in this protein. This is discussed in more detail later.

Transient dimerization

It is known that weak protein self-association can cause exchange broadening (Pfuhl et al. 1999) and give rise to dispersion effects. Here we consider the feasibility of this scenario for Ln^{3+}-NcTnC. In particular, we suggest that *intermolecular* pseudocontact shifts can come into play in this system, consistent with the increase in dispersion amplitudes along the series La^{3+}-Ce^{3+}-Pr^{3+}.

EF-hand domains are known for their tendency to form dimers. The standard arrangement in the EF-hand homodimers is such that the N-terminal helices from the two monomeric units pack against each other in antiparallel fashion, and likewise the C-terminal helices pack against each other in antiparallel fashion (Brodersen et al. 1998). The resulting pattern resembles a hash mark (#). A search of the Protein Data Bank (Berman et al. 2000) turned up 19 such structures (this number includes apo, Ca^{2+}-loaded, and Ln^{3+}-loaded proteins, with structures solved both by X-ray (Mittl et al. 2002; Strynadka et al. 1997) and NMR spectroscopy (Potts et al. 1995; Drohat et al. 1999)). For Ca^{2+}-NcTnC the evidence of weak self-association (K_D = 7 mM) has been obtained from ^{15}N linewidth measurements (Spyracopoulos et al. 2001).

To probe self-association effects in the lanthanide-loaded NcTnC we carried out the diffusion measurements using the ^{15}N-filtered pulsed field gradient experiment (Choy et al. 2002). The data for a series of samples are illustrated in Fig. S1 and the results are summarized in Table 1. As can be seen from Table 1, the apo form of NcTnC shows substantial aggregation, which is somewhat alleviated when the sample is loaded with up to one molar equivalent of Ca^{2+} or Ln^{3+} ion. Subsequently, when the excess of an ion is introduced in the solution, the difference emerges between Ca^{2+} and Ln^{3+}: the former shifts the equilibrium strongly toward the monomer, while the latter promotes aggregation.

The data listed in Table 1 have been used to estimate a fraction of dimers in solutions of Ln^{3+}-NcTnC. As a first step, we employed HYDROPRO (de la Torre et al. 2000) to calculate the translational diffusion coefficients for the set of 19 EF-hand domain homodimers found in the Protein Data Bank. This calculation led to the average ratio $D_t^{\text{monomer}}/D_t^{\text{dimer}} = 1.20$. Using this ratio and assuming that $D_t^{\text{monomer}} = 8.61 \cdot 10^{-7}\text{cm}^2/\text{s}$ (see Table 1) we estimated the fraction of dimers in each of our samples. For example, it has been found that the Pr^{3+}-NcTnC sample in the absence of salt contains 55% of the dimeric form, whereas in the presence of salt the fraction of dimer drops to 15% (cf. two rows at the bottom of Table 1).

These estimates can be readily tested against the ^{15}N relaxation parameters. Assuming that $D_{\text{rot}}^{\text{dimer}}/D_{\text{rot}}^{\text{monomer}} = 1.90$ (Daragan and Mayo 1997), we predicted that the addition of salt to the Pr^{3+}-NcTnC sample should sharpen the spectral lines by ca. 25%. Indeed, the addition of 100 mM NaCl caused uniform sharpening of the troponin resonances, with a 23% average reduction in the ^{15}N linewidth. Thus we are reasonably confident that our estimates correctly characterize the monomer–dimer equilibrium in lanthanide-loaded samples of NcTnC.

Table 1 Translational diffusion coefficients in solutions of NcTnC

Loading ion content [molar equivalents NcTnC]	D_t[a] [10^{-7} cm^2/s]	Sample conditions[b]
0.0	7.92 ± 0.03	1.2 mM ^2H,^{15}N-NcTnC
1.0 (Ca^{2+})	8.15 ± 0.04	1.3 mM ^2H,^{15}N-NcTnC
4.0 (Ca^{2+})	8.46 ± 0.10 [c]	1.3 mM ^2H,^{15}N-NcTnC
4.0 (Ca^{2+})	8.61 ± 0.05 [d]	1.3 mM ^2H,^{15}N-NcTnC; 100 mM NaCl [e]
1.25 (La^{3+})	8.28 ± 0.03	0.15 mM ^2H,^{15}N-NcTnC
1.25 (La^{3+})	7.82 ± 0.03	1.8 mM ^2H,^{15}N-NcTnC
0.8 (Ce^{3+})	8.09 ± 0.05	0.9 mM ^2H,^{15}N-NcTnC
1.25 (Ce^{3+})	7.84 ± 0.04	2.0 mM ^{13}C,^{15}N-NcTnC
1.25 (Pr^{3+})	7.79 ± 0.07	2.0 mM ^{13}C,^{15}N-NcTnC
1.25 (Pr^{3+})	8.37 ± 0.07	1.8 mM ^2H,^{15}N-NcTnC; 100 mM NaCl

[a] The errors are determined by a jackknife method where two of the seven measured points (Fig. S1), are randomly discarded

[b] Other sample conditions are as described in the Materials and methods. Of note, addition of $LnCl_3$ aliquot produces turbid clouds in the solution of NcTnC. After approximately one minute of shaking, the sample returns to its original lucid state. This effect can be attributed to transient protein aggregation caused by a local excess of Ln^{3+} ions, consistent with the data presented in this table. Large excess of Ln^{3+} ions, above 2.5 molar equivalents, cause the protein to crash out of solution. None of this behavior has been observed in the Ca^{2+}-loaded samples

[c] Assuming $D_t^{\text{monomer}} = 8.61 \cdot 10^{-7}\text{cm}^2/\text{s}$, $D_t^{\text{monomer}}/D_t^{\text{dimer}} = 1.20$ (see text) we obtain for this sample K_D= 9 mM. This is in good agreement with the previously reported result. K_D= 7 mM (Spyracopoulos et al. 2001)

[d] The calculation by HYDROPRO (de la Torre et al. 2000) using the structure of Ca^{2+}-NcTnC (mean coordinates 1AP4) yields the value $D_t = 8.54 \cdot 10^{-7}\text{cm}^2/\text{s}$

[e] The effect of 100 mM NaCl on viscosity of the solution is negligible (Kestin et al. 1981)

Certain tentative suggestions can be made about a structure of the Ln^{3+}-NcTnC dimer. While NcTnC is distinct from most EF-hand domains in that it has an extra helix, its structure also permits a #-type arrangement found in the other EF-hand homodimers (illustrated in Fig. S2). Of note, this model predicts that the C-terminal residues from one monomeric unit are positioned near the metal-binding site of the other unit (and vice versa). This explains the disappearance of resonances 85–89 (86–89) in the samples loaded with Pr^{3+} (Ce^{3+}), see Fig. 4. The peaks in question are likely obliterated by the intermolecular paramagnetic relaxation and by the Ln^{3+}-induced exchange broadening. Apart from several C-terminal residues, the model shown in Fig. S2 does not predict any appreciable intermolecular contributions to pseudocontact shifts or to paramagnetic relaxation. This is also consistent with our observations and, in particular, with the fact that the experimental δ_{pc} data can be successfully fitted using the monomeric structure of NcTnC, Fig. 2.

The important question remains: is it possible that monomer–dimer exchange in the Ln^{3+}-NcTnC samples is responsible for the observed relaxation dispersion behavior? To address this question let us assume that monomer and dimer are characterized by two distinct sets of shifts, δ^a and δ^b. In this situation the observed shifts, $p_a\delta^a + p_b\delta^b$, are a function of the monomer-dimer equilibrium. By utilizing the samples with different p_a/p_b, we can estimate $\Delta\delta = \delta^a - \delta^b$ and thus try to determine whether the monomer–dimer exchange can be a cause of the experimentally observed dispersions.

As it turns out, the change in p_a/p_b brings very little variation in the observed shifts. For instance, the addition of 100 mM NaCl to the Pr^{3+}-NcTnC sample alters the monomer-dimer equilibrium from 45:55 to 85:15. At the same time, the $^1H^N$ spectral frequencies change only marginally (the largest shift 0.055 ppm, the second largest shift 0.035 ppm). Likewise, 10-fold dilution has little effect on the observed shifts: in dilute Pr^{3+} and La^{3+} samples the shifts change by less than 0.040 ppm compared to the concentrated samples. The pseudocontact shifts also remain essentially unchanged. These observations lead us to conclude that $\Delta\delta = \delta^a - \delta^b$ is small and, therefore, cannot be held responsible for the observed dispersion effects (in fact, our estimates show that $\Delta\delta$ falls an order of magnitude short).

This result is not so surprising from the structural standpoint. Indeed, it is often the case that formation of a dimer causes only limited changes in $^1H^N$ chemical shifts. We also do not expect to see much change in pseudocontact shifts, assuming that the structure of the dimer is as shown in Fig. S2.

The above analysis suggests that monomer–dimer exchange is unlikely to be the primary factor behind the observed dispersion effects. However, it is possible that dimerization affects the dispersion behavior indirectly. For instance, dimerization may alter the time scale of the internal motion in the Ln^{3+}-binding site or the time scale of the opening/closing dynamics. To test this possibility, we recorded the relaxation dispersion data on the 100 mM NaCl Pr^{3+}-NcTnC sample, where the dimerization is largely suppressed (600 MHz only, data not shown). Indeed, it turned out that the τ_{ex} in this sample are approximately 2-fold longer than in the sample that contains no salt. The details of weak self-association in Ca^{2+}-NcTnC and the influence of this process on the exchange broadening are currently under investigation in Sykes' group (Julien and Sykes, personal communication).

Ln^{3+} on-off exchange

It has been demonstrated that the on-off exchange of the bound ion can give rise to relaxation dispersion effects in proteins (Millet et al. 2002). In the case of Ln^{3+}-loaded samples, such exchange would automatically lead to modulation of pseudocontact shifts. In this section we argue that ion on-off exchange is unlikely to play any significant role with regard to the dispersion effects observed in the present study.

To determine the metal ion k_{off} rates, we analyzed the titration data from Ce^{3+} and Pr^{3+} samples (30 and 10°C, respectively). Specifically, in the series of ^1H,^{15}N-HSQC spectra we selected several well resolved peak pairs from apo-NcTnC and Ln^{3+}-NcTnC. For each of the apo peaks we monitored the broadening of the spectral line as a function of the lanthanide concentration. The linewidth data were fitted using the Bloch-McConnell equation (McConnell 1958), where the frequency separation between the apo- and holo-resonances was taken directly from the spectra. The extracted off-rates were 5–10 and 15–25 s^{-1}at 10°C and 30°C, respectively.[4]

To minimize the effects of on-off exchange, the samples used for the dispersion measurements were

[4] During the course of titration apo peaks behave exactly as expected, i.e. undergo gradual broadening to the point of complete disappearance. Holo peaks, on the other hand, do not show the expected sharpening trend. This unusual behavior can be explained if one recalls that the addition of Ln^{3+} promotes protein aggregation, which leads to longer τ_R and increased dipolar relaxation. Furthermore, the excess of Ln^{3+} brings about translational paramagnetic relaxation. The behavior of the holo peaks is therefore rather complex and does not lend itself to a quantitative interpretation.

loaded with 1.25 molar equivalents of La^{3+}, Ce^{3+}, and Pr^{3+}. The excess of lanthanide ensures that the fraction of apo-NcTnC is vanishingly small and, therefore, the exchange broadening is minimal. Using the determined value for k_{off}, 10 s^{-1} at 10°C, and assuming that k_{on} is diffusion-controlled, as it is for calcium (Hazard et al. 1998; Li et al. 2002), we estimated that the R_{ex} contribution from the on-off exchange under these conditions does not exceed 0.2 s^{-1}. The small term of this magnitude can be safely ignored.

We can also approach this problem from another direction. Assume for a moment that the observed dispersion effects are due to the Ln^{3+} on-off exchange. Using the values of τ_{ex} derived from the dispersion data (Fig. 5) and evaluating the relationships $\tau_{ex}^{-1} = k_{on}[Ln^{3+}] + k_{off}$ and $k_{off}/k_{on} = [NcTnC][Ln^{3+}]/[Ln^{3+}\text{-NcTnC}]$ we can find k_{on} and the concentrations of apo and holo species in the sample. Based on these data, the R_{ex} contributions can be back-calculated. As it turns out, the R_{ex} values so obtained fall two orders of magnitude short of the experimentally measured values, which again demonstrates that the on-off exchange is not a principal cause of the dispersion effects.

As a final control, the dispersion measurements were repeated using an additional sample loaded with 0.8 molar equivalents of Ce^{3+} (600 MHz only, data not shown). In this sample, the contribution of on-off exchange to the transverse relaxation rate is expected to be approximately equal to k_{off}. The dispersion profiles recorded with this sample are in agreement, within error margin, with the main body of dispersion data.

On-off exchange involving secondary Ln^{3+} binding sites

In principle, it could be suggested that NcTnC has some additional low-affinity Ln^{3+} binding sites which could play a role in Ln^{3+}-induced dispersions. There is, however, no factual basis for this hypothesis. In the case of Ca^{2+}, no secondary binding has been observed in the thorough titration studies (Li et al. 1997). Likewise, Ce^{3+} and Pr^{3+} titration data contain no evidence of secondary binding. While some of the resonances drift slightly (up to 0.05 ppm in proton dimension) as the concentration of the lanthanide ion is raised from 1.0 to 1.5 molar equivalents, there are no dramatic shifts and all the peaks are accounted for throughout the titration. Finally, the control measurements conducted at 0.8 molar equivalents of Ce^{3+} confirmed that the presence of excess lanthanide ions has no impact on the observed dispersions.

Relevance for structural analyses

The conformational state of the EF-hand pair is determined by three elements: two calcium-binding sites and the 2-helix element that straddles them. These elements are all structurally coupled. The sites are coupled with each other through a stretch of antiparallel β-sheet comprised of two residues (both residues are in position 8 of the canonical calcium-binding motif). They are also coupled to the 2-helix unit, with the C-terminal residue of site I (conserved Glu in position 12) and the N-terminal residue of site II (Asp or other residue in position 1) largely responsible for reorientation of this unit in response to ion binding (Grabarek 2006).

This assembly, termed 'EFβ-scaffold', displays substantial conformational diversity. For example, the orientation of the 2-helix element varies among different members of EF family, giving rise to the ''conformational continuum'' (Yap et al. 1999). Individual proteins also demonstrate conformational variability – for example, the N-terminal domain of calmodulin (NCaM) occurs not only in closed and open forms, but also in a semi-open form (Chou et al. 2001; Fallon and Quiocho 2003). A disulphide-linked variant of NCaM shows an unusual Ca^{2+}-binding mode where Glu in position 12 is not involved in coordinating the ion. It has been suggested that this conformation is also represented in the kinetic pathway of the native protein (Grabarek 2005).

With their predisposition to conformational heterogeneity, proteins such as CaM and TnC show the pattern of exchange broadening in the NMR spectra. The broadening generally occurs in and around the calcium-binding sites, but not in the 2-helix unit. In Ca^{2+}-NcTnC, ^{15}N line broadening has been previously noted for residues 28, 37, 39, 40, 61, and 64 (Pääkkönen et al. 1998), in agreement with our data. In apo-CCaM, ^{15}N relaxation and relaxation dispersion experiments identified a number of residues affected by conformational exchange (Malmendal et al. 1999; Tjandra et al. 1995). If these data are mapped onto NcTnC (by aligning sites I of the two proteins), the residues 22, 23, 26, 28, 35, and 36 in and around the defunct binding site of NcTnC are predicted to be dynamic. In $(Ca^{2+})_2$-E140Q-CCaM, both binding sites show extensive broadening which has been linked to the opening/closing motion (Evenäs et al. 2001; Lundström and Akke 2004). In particular, the largest exchange effects have been observed in the two β-sheet residues that form the bridge between the two calcium-binding sites.

Our data demonstrate an interesting complementarity effect in the μs time-scale motion of the

calcium-binding loops. In the Ca^{2+}-NcTnC sample, site I (defunct) is highly mobile, while site II (functional) is not, although the flanking residues immediately outside the calcium-binding loop show motion. In La^{3+}-NcTnC the situation is reversed: the entire site II is mobile, but the motion in and around site I is considerably reduced. This is an interesting example of what can be called 'dynamic anti-cooperativity' in the pair of EF-hand motifs. From this perspective it is logical that the motions in Ca^{2+}- and Ln^{3+}-NcTnC occur on the same time scale (Fig. 5) as this time scale appears to be 'programmed' in the structure of the EFβ-scaffold. Dynamic coupling between the two calcium-binding sites have been noted before in ^{15}N relaxation studies of fast (ps-ns) motions (Akke et al. 1993; Spyracopoulos et al. 1998; Marchand and Roux 1998).

It is also noteworthy that the internal dynamics influences the affinity of the EF-hand site for the Ca^{2+} or Ln^{3+} ion. Based on the binding constants, the free energy difference between Ca^{2+}- and La^{3+}-NcTnC is estimated to be ca. 1–2 kcal/mol. The gain in enthalpy due to the electrostatic interactions is, however, much larger (Mustafi et al. 2004; Dudev et al. 2005). The balance is provided by entropy, which mainly stems from solvation/desolvation of the ions, but also reflects the change in internal dynamics of the protein.

Concluding remarks: Ln^{3+} ions as a probe of μs–ms dynamics

Ideally, we would like to see Ln^{3+} as a non-intrusive probe of μs–ms protein dynamics. In this desired scenario, Ln^{3+} binds tightly to a well-defined rigid binding site. In doing so, it provides a perfect substitute for calcium, preserving both the structure and dynamics of the physiologically-relevant Ca^{2+}-loaded form. When bound, Ln^{3+} induces pseudocontact shifts across a large swath of protein structure. If there is μs–ms internal motion in the covered area, the involved spins experience modulation of pseudocontact shifts. As a result, the dispersion effects are amplified, or even created, for these spins.

In reality, however, we are faced with some contradictory choices. Among calcium-binding proteins we distinguish (i) the buffers and (ii) the sensor proteins. The buffers, such as parvalbumin, typically possess rigidly structured high-affinity binding sites (Corson et al. 1983), but feature little or none of μs–ms dynamics (Baldellon et al. 1998). Conversely, sensor proteins, such as NcTnC, display rich and functionally important dynamic behavior. However, by their very nature they are finely tuned for regulation by calcium. As a result, the Ln^{3+}-for-Ca^{2+} substitution can be no longer considered perturbation-free. The assumption of a rigid binding site can also be called into question, as demonstrated in this study.

It is still feasible that this approach can work well for calcium-binding proteins. For instance, it can be envisaged that μs–ms motions in multidomain proteins can be investigated in this manner by utilizing long-range pseudocontact shifts (Bertini et al. 2004). However, a more general approach is clearly desirable. We propose that the use of lanthanide-binding tags attached to the protein surface can provide a good solution. There are obvious advantages to this approach: (i) the Ln^{3+} probe can be introduced into proteins other than calcium-binding proteins, (ii) the tag can be positioned such that it provides good coverage of the dynamic site and at the same time does not interfere with the motion, (iii) the tags bind Ln^{3+} with high affinity and the coordination geometry is usually well characterized.

To explore this strategy we carried out some preliminary studies on NcTnC. A number of single-cysteine variants of NcTnC have been prepared, tagged with MTS-EDTA (Ikegami et al. 2004), and loaded with ions (with Ln^{3+} bound to a tag and Ca^{2+} bound to NcTnC). Of these mutants, S84C produced a poorly resolved spectrum suggestive of conformational heterogeneity. It is likely that in this case the tag interfered with protein opening/closing. On the contrary, T13C and D75C samples showed bona fide spectra. It turned out, however, that pseudocontact shifts in these spectra were small (less than 0.1 ppm for Yb^{3+}-loaded tags). Furthermore, signal-to-noise ratio proved to be poor (presumably because of intermolecular Curie spin relaxation). As a result, these samples were unsuitable for observations of Ln^{3+}-induced dispersions.

The main difficulty with the use of MTS-EDTA tags stems from the length and the flexibility of the linker. The 'swaying' motion of the tag is effective in averaging out pseudocontact shifts in the protein (Dvoretsky et al. 2002; Ikegami et al. 2004). Shorter and more constrained tags can produce larger pseudocontact shifts. Recently, a number of new tags have been developed that demonstrated good-quality spectra and pseudocontact shifts as large as 1 ppm (Ikegami et al. 2004; Prudêncio et al. 2004; Haberz et al. 2006). The use of these improved tags should facilitate the studies of Ln^{3+}-induced dispersions.

Use of Ln^{3+} ions in relaxation dispersion studies offers some interesting possibilities. First, long-range pseudocontact shifts can generate large dispersions where chemical shifts fail. This happens, for example, when the motion involves a translocation of a 'rigid'

structural unit, such as α-helix. The local environment of the spins residing in such rigid fragment does not change and therefore there is no change in chemical shifts. Pseudocontact shifts, on the other hand, can be efficiently modulated when the fragment of interest moves relative to the Ln^{3+}-binding site—thus generating the dispersion. The second and more important advantage stems from a simple relationship between pseudocontact shifts and structural variables. In the case of chemical shifts, it is generally difficult to translate $\Delta\omega$ values derived from the dispersions data into structural information (Hill et al. 2000; Skrynnikov et al. 2002; Korzhnev et al. 2004). In contrast, if $\Delta\omega$ originates from pseudocontact shifts then structural interpretation can be more straightforward. In conclusion, Ln^{3+}-induced dispersions, demonstrated for the first time in this study, could become a useful addition to a growing collection of methods for studying μs–ms protein dynamics.

Materials and methods

The NcTnC (C35S/C84S variant) was expressed and purified as described previously (Li et al. 1995; Eichmüller and Skrynnikov 2005). The spectral assignment experiments were conducted on the samples of ^{13}C,^{15}N-labeled NcTnC (1.2–2.0 mM protein concentration). The relaxation dispersion measurements were conducted on samples of ^{2}H,^{15}N-labeled NcTnC (1.8 mM protein concentration). All samples were loaded with 1.25 molar equivalents of $LnCl_3$. The solvent composition was 90:10 H_2O:D_2O, 10 mM imidazole, 0.01% NaN_3, pH 7 (prior to Ln^{3+} titration). The S84C, T13C, and D75C mutants were constructed using the Stratagene QuikChange system. The tags were attached to cysteine thiol groups by incubating the samples overnight with MTS-EDTA (Toronto Research Chemicals). The presence of the Ln^{3+}-loaded tag was confirmed by MALDI-TOF mass spectrometry. The sample conditions were 1.2–1.6 mM tagged protein, 1.0 molar equivalent Ln^{3+}, 4.0 molar equivalents Ca^{2+}, 150 mM NaCl, solvent as described above.

Backbone assignments of Ln^{3+}-NcTnC were obtained from a standard suite of triple-resonance experiments including HNCACB, CBCA(CO)NH, HN(CA)CO, and HNCO (Kay 1995; Sattler et al. 1999) executed at 600 MHz Varian Unity Inova spectrometer at 30°C. The assignment was transferred to 10°C by means of the 'temperature titration' using ^{15}N,^{1}H-HSQC and HNCO experiments. The data were processed and analyzed using NMRPipe (Delaglio et al. 1995), NMRView (Johnson and Blevins 1994), and Sparky (Goddard and Kneller 2002) software. The relaxation dispersion experiments and the data fitting procedure have been described previously (Eichmüller and Skrynnikov 2005). The dispersions data were collected at 12.4°C on Varian Unity Inova 600 and 800 MHz spectrometers equipped with room-temperature and cryogenic probes, respectively. The proton spin-lock field strengths varied from 1.13 (1.05) to 12.38 (11.75) kHz in the measurements at 600 (800) MHz. Each data set, collected in 27 h, was comprised of 6 reference spectra with $t_{rel} = 0$ and 16 spectra with $t_{rel} = T = 50$ ms sampling 8 different spin lock strengths. The Ca^{2+}-NcTnC data are as reported in our recent communication (Eichmüller and Skrynnikov 2005). Because of the data processing error, the 600 MHz dispersion profiles shown in Fig. 5 of that paper are shifted upward by a constant amount relative to their correct positions. This has strictly no impact on the analyses of slow motions as the shift is absorbed into $R_{anti}^{600} - R_{zz}^{600}$. The curves shown in the top panels of Fig. 3 in this work are correct.

The translational diffusion data were obtained from a ^{15}N-filtered pulsed field gradient experiment (Choy et al. 2002) executed in 1D mode. The measurement time was 3 h per sample. Gradient strengths were calibrated as described by Price (1998). The signals from the amide region were integrated using Varian VNMR software and the obtained integral intensities were analyzed as a function of gradient strengths as illustrated in Fig. S1. The HYDROPRO (de la Torre et al. 2000) calculations were performed assuming the temperature 10 °C and the corresponding solvent viscosity, 1.307 cP. In calculating the diffusion parameters we also used a randomly-selected control group consisting of 10 high-resolution structures of small dimeric proteins which produced the average value $D_t^{monomer}/D_t^{dimer} = 1.23$.

Acknowledgements We gratefully thank Lewis Kay for his insights, advice, and encouragement, Brian Sykes for the kind gift of the expression vector, Monica Li, Grant Gay, and Olivier Julien for useful discussions, and Jun Xu for the help with spectral assignments. Some of the measurements were conducted at the National Magnetic Resonance Facility at Madison. This work was supported by Max Kade Foundation research grant to C. E. and NSF CAREER grant 044563 to N. R. S.

References

Akke M, Skelton NJ, Kördel J, Palmer AG, Chazin WJ (1993) Effects of ion binding on the backbone dynamics of calbindin-D_{9k} determined by ^{15}N NMR relaxation. Biochemistry 32:9832–9844

Allegrozzi M, Bertini I, Choi SN, Lee YM Luchinat C (2002) Detecting small structural changes in metalloproteins by the

use of NMR pseudocontact shifts. Eur J Inorg Chem 2121–2127

Baig I, Bertini I, Del Bianco C, Gupta YK, Lee YM, Luchinat C, Quattrone A (2004) Paramagnetism-based refinement strategy for the solution structure of human alpha-parvalbumin. Biochemistry 43:5562–5573

Baldellon C, Alattia JR, Strub MP, Pauls T, Berchtold MW, Cave A, Padilla A (1998) ^{15}N NMR relaxation studies of calcium-loaded parvalbumin show tight dynamics compared to those of other EF-hand proteins. Biochemistry 37:9964–9975

Banci L, Bertini I, Bren KL, Cremonini MA, Gray HB, Luchinat C, Turano P (1996) The use of pseudocontact shifts to refine solution of paramagnetic metalloproteins: Met80Ala cyanocytochrome c as an example. J Biol Inorg Chem 1:117–126

Bentrop D, Bertini I, Cremonini MA, Forsén S, Luchinat C, Malmendal A (1997) Solution structure of the paramagnetic complex of the N-terminal domain of calmodulin with two Ce^{3+} ions by ^{1}H NMR. Biochemistry 36:11605–11618

Berman HM, Westbrook J, Feng Z, Gilliland G, Bhat TN, Weissig H, Shindyalov IN, Bourne PE (2000) The Protein Data Bank. Nucl Acids Res 28:235–242

Bertini I, Carrano CJ, Luchinat C, Piccioli N, Poggi L (2002) A ^{15}N NMR mobility study on the dicalcium P43M calbindin D_{9k} and its mono-La^{3+}-substituted form. Biochemistry 41:5104–5111

Bertini I, Del Bianco C, Gelis I, Katsaros N, Luchinat C, Parigi G, Peana M, Provenzani A, Zoroddu MA (2004) Experimentally exploring the conformational space sampled by domain reorientation in calmodulin. Proc Natl Acad Sci USA 101:6841–6846

Bertini I, Donaire A, Jiménez B, Luchinat C, Parigi G, Piccioli M, Poggi L (2001a) Paramagnetism-based versus classical constraints: an analysis of the solution structure of Ca·Ln·calbindin D_{9k}. J Biomol NMR 21:85–98

Bertini I, Janik MBL, Lee YM, Luchinat C, Rosato A (2001b) Magnetic susceptibility tensor anisotropies for a lanthanide ion series in a fixed protein matrix. J Am Chem Soc 123:4181–4188

Bertini I, Luchinat C, Parigi G (2001c) Solution NMR of paramagnetic molecules. Elsevier, Amsterdam

Biekofsky RR, Muskett FW, Schmidt JM, Martin SR, Browne JP, Bayley PM, Feeney J (1999) NMR approaches for monitoring domain orientations in calcium-binding proteins in solution using partial replacement of Ca^{2+} by Tb^{3+}. FEBS Lett 460:519–526

Bloom M, Reeves LW, Wells EJ (1965) Spin echoes and chemical exchange. J Chem Phys 42:1615–1624

Brodersen DE, Etzerodt M, Madsen P, Celis JE, Thøgersen HC, Nyborg J, Kjeldgaard M (1998) EF-hands at atomic resolution: the structure of human psoriasin (S100A7) solved by MAD phasing. Struct Fold Des 6:477–489

Burling FT, Weis WI, Flaherty KM, Brunger AT (1996) Direct observation of protein solvation and discrete disorder with experimental crystallographic phases. Science 271:72–77

Campbell ID, Dobson CM, Williams RJP (1975) Nuclear magnetic resonance studies on structure of lysozyme in solution. Proc R Soc Lond A 345:41–59

Chou JJ, Li SP, Klee CB, Bax A (2001) Solution structure of Ca^{2+}-calmodulin reveals flexible hand-like properties of its domains. Nat Struct Biol 8:990–997

Choy WY, Mulder FAA, Crowhurst KA, Muhandiram DR, Millett IS, Doniach S, Forman-Kay JD, Kay LE (2002) Distribution of molecular size within an unfolded state ensemble using small-angle X-ray scattering and pulse field gradient NMR techniques. J Mol Biol 316:101–112

Contreras MA, Ubach J, Millet O, Rizo J, Pons M (1999) Measurement of one bond dipolar couplings through lanthanide-induced orientation of a calcium-binding protein. J Am Chem Soc 121:8947–8948

Corson DC, Williams TC, Sykes BD (1983) Calcium-binding proteins - optical stopped-flow and proton nuclear magnetic resonance studies of the binding of the lanthanide series of metal ions to parvalbumin. Biochemistry 22:5882–5889

Daragan VA, Mayo KH (1997) Motional model analyses of protein and peptide dynamics using ^{13}C and ^{15}N NMR relaxation. Prog NMR Spectrosc 31:63–105

de la Torre JG, Huertas ML, Carrasco B (2000) Calculation of hydrodynamic properties of globular proteins from their atomic-level structure. Biophys J 78:719–730

Delaglio F, Grzesiek S, Vuister GW, Zhu G, Pfeifer J, Bax A (1995) NMRPipe – a multidimensional spectral processing system based on unix pipes. J Biomol NMR 6:277–293

Desvaux H, Birlirakis N, Wary C, Berthault P (1995) Study of slow molecular motions in solution using off-resonance irradiation in homonuclear NMR 2. Fast chemical exchange processes. Mol Phys 86:1059–1073

Deverell C, Morgan RE, Strange JH (1970) Studies of chemical exchange by nuclear magnetic relaxation in the rotating frame. Mol Phys 18:553–559

Drohat AC, Tjandra N, Baldisseri DM, Weber DJ (1999) The use of dipolar couplings for determining the solution structure of rat apo-S100B($\beta\beta$). Protein Sci 8:800–809

Dudev T, Chang LY, Lim C (2005) Factors governing the substitution of La^{3+} for Ca^{2+} and Mg^{2+} in metalloproteins: a DFT/CDM study. J Am Chem Soc 127:4091–4103

Dvoretsky A, Gaponenko V, Rosevear PR (2002) Derivation of structural restraints using a thiol-reactive chelator. FEBS Lett 528:189–192

Dwek RA, Richards RE, Morallee KG, Nieboer E, Williams RJ, Xavier AV (1971) Lanthanide cations as probes in biological systems – proton relaxation enhancement studies for model systems and lysozyme. Eur J Biochem 21:204–217

Eichmüller C, Skrynnikov NR (2005) A new amide proton $R_{1\rho}$ experiment permits accurate characterization of microsecond time-scale conformational exchange. J Biomol NMR 32:281–293

Evenäs J, Forsén S, Malmendal A, Akke M (1999) Backbone dynamics and energetics of a calmodulin domain mutant exchanging between closed and open conformations. J Mol Biol 289:603–617

Evenäs J, Malmendal A, Akke M (2001) Dynamics of the transition between open and closed conformations in a calmodulin C-terminal domain mutant. Struct Fold Des 9:185–195

Fallon JL, Quiocho FA (2003) A closed compact structure of native Ca^{2+}-calmodulin. Struct Fold Des 11:1303–1307

Farah CS, Miyamoto CA, Ramos CHI, Dasilva ACR, Quaggio RB, Fujimori K, Smillie LB, Reinach FC (1994) Structural and regulatory functions of the NH_2- and COOH-terminal regions of skeletal-muscle troponin I. J Biol Chem 269:5230–5240

Gaponenko V, Abusamhadneh E, Abbott MB, Finley N, Gasmi-Seabrook G, Solaro RJ, Rance M, Rosevear PR (1999) Effects of troponin I phosphorylation on conformational exchange in the regulatory domain of cardiac troponil C. J Biol Chem 274:16681–16684

Gay GL, Lindhout DA, Sykes BD (2004) Using lanthanide ions to align troponin complexes in solution: order of lanthanide occupancy in cardiac troponin C. Protein Sci 13:640–651

Goddard TD, Kneller DG (2002) SPARKY3. University of California, San Francisco

Grabarek Z (2005) Structure of a trapped intermediate of calmodulin: Calcium regulation of EF-hand proteins from a new perspective. J Mol Biol 346:1351–1366

Grabarek Z (2006) Structural basis for diversity of the EF-hand calcium-binding proteins. J Mol Biol 359:509–525

Guéron M (1975) Nuclear relaxation in macromolecules by paramagnetic ions – novel mechanism. J Magn Reson 19:58–66

Haberz P, Rodriguez-Castañeda F, Junker J, Becker S, Leonov A, Griesinger C (2006) Two new chiral EDTA-based metal chelates for weak alignment of proteins in solution. Org Lett 8:1275–1278

Hazard AL, Kohout SC, Stricker NL, Putkey JA, Falke JJ (1998) The kinetic cycle of cardiac troponin C: Calcium binding and dissociation at site II trigger slow conformational rearrangements. Protein Sci 7:2451–2459

Hill RB, Bracken C, DeGrado WF, Palmer AG (2000) Molecular motions and protein folding: Characterization of the backbone dynamics and folding equilibrium of α_2D using ^{13}C NMR spin relaxation. J Am Chem Soc 122:11610–11619

Ikegami T, Verdier L, Sakhaii P, Grimme S, Pescatore B, Saxena K, Fiebig KM, Griesinger C (2004) Novel techniques for weak alignment of proteins in solution using chemical tags coordinating lanthanide ions. J Biomol NMR 29:339–349

Ishima R, Wingfield PT, Stahl SJ, Kaufman JD, Torchia DA (1998) Using amide ^{1}H and ^{15}N transverse relaxation to detect millisecond time-scale motions in perdeuterated proteins: application to HIV-1 protease. J Am Chem Soc 120:10534–10542

John M, Park AY, Pintacuda G, Dixon NE, Otting G (2005) Weak alignment of paramagnetic proteins warrants correction for residual CSA effects in measurements of pseudocontact shifts. J Am Chem Soc 127:17190–17191

Johnson BA, Blevins RA (1994) NMRView – a computer program for the visualization and analysis of NMR data. J Biomol NMR 4:603–614

Kay LE (1995) Pulsed field gradient multi-dimensional NMR methods for the study of protein structure and dynamics in solution. Prog Biophys Mol Biol 63:277–299

Kestin J, Khalifa HE, Correia RJ (1981) Tables of the dynamic and kinematic viscosity of aqueous NaCl solutions in the temperature range 20–150°C and the pressure range 0.1–35 MPa. J Phys Chem Ref Data 10:71–87

Kobayashi T, Solaro RJ (2005) Calcium, thin filaments, and the integrative biology of cardiac contractility. Annu Rev Physiol 67:39–67

Korzhnev DM, Salvatella X, Vendruscolo M, Di Nardo AA, Davidson AR, Dobson CM, Kay LE (2004) Low-populated folding intermediates of Fyn SH3 characterized by relaxation dispersion NMR. Nature 430:586–590

Kumar VD, Lee L, Edwards BFP (1991) Refined crystal structure of ytterbium-substituted carp parvalbumin 4.25 at 1.5 Å, and its comparison with the native and cadmium-substituted structures. FEBS Lett 283:311–316

Lee L, Sykes BD (1983) Use of lanthanide-induced nuclear magnetic resonance shifts for determination of protein structure in solution – EF calcium-binding site of carp parvalbumin. Biochemistry 22:4366–4373

Li MX, Gagné SM, Spyracopoulos L, Kloks CPAM, Audette G, Chandra M, Solaro RJ, Smillie LB, Sykes BD (1997) NMR studies of Ca^{2+} binding to the regulatory domains of cardiac and E41A skeletal muscle troponin C reveal the importance of site I to energetics of the induced structural changes. Biochemistry 36:12519–12525

Li MX, Gagné SM, Tsuda S, Kay CM, Smillie LB, Sykes BD (1995) Calcium binding to the regulatory N-domain of skeletal-muscle troponin C occurs in a stepwise manner. Biochemistry 34:8330–8340

Li MX, Saude EJ, Wang X, Pearlstone JR, Smillie LB, Sykes BD (2002) Kinetic studies of calcium and cardiac troponin I peptide binding to human cardiac troponin C using NMR spectroscopy. Eur Biophys J 31:245–256

Li MX, Spyracopoulos L, Sykes BD (1999) Binding of cardiac troponin-$I_{147–163}$ induces a structural opening in human cardiac tropoin C. Biochemistry 38:8289–8298

Li Y, Love ML, Putkey JA, Cohen C (2000) Bepridil opens the regulatory N-terminal lobe of cardiac troponin C. Proc Natl Acad Sci USA 97:5140–5145

Likic VA, Strehler EE, Gooley PR (2003) Dynamics of Ca^{2+}-saturated calmodulin D129N mutant studied by multiple molecular dynamics simulations. Protein Sci 12:2215–2229

Lundström P, Akke M (2004) Quantitative analysis of conformational exchange contributions to ^{1}H-^{15}N multiple-quantum relaxation using field-dependent measurements. Time scale and structural characterization of exchange in a calmodulin C-terminal domain mutant. J Am Chem Soc 126:928–935

Luo Y, Wu JL, Li B, Langsetmo K, Gergely J, Tao T (2000) Photocrosslinking of benzophenone-labeled single cysteine troponin I mutants to other thin filament proteins. J Mol Biol 296:899–910

Machonkin TE, Westler WM, Markley JL (2002) ^{13}C{^{13}C} 2D NMR: a novel strategy for the study of paramagnetic proteins with slow electronic relaxation rates. J Am Chem Soc 124:3204–3205

Malmendal A, Evenäs J, Forsén S, Akke M (1999) Structural dynamics in the C-terminal domain of calmodulin at low calcium levels. J Mol Biol 293:883–899

Marchand S, Roux B (1998) Molecular dynamics study of calbindin D_{9k} in the apo and singly and doubly calcium-loaded states. Proteins 33:265–284

McConnell HM (1958) Reaction rates by nuclear magnetic resonance. J Chem Phys 28:430–431

McDermott AE (2004) Structural and dynamic studies of proteins by solid-state NMR spectroscopy: rapid movement forward. Curr Opin Struc Biol 14:554–561

McKay RT, Saltibus LF, Li MX, Sykes BD (2000) Energetics of the induced structural change in a Ca^{2+} regulatory protein: Ca^{2+} and troponin I peptide binding to the E41A mutant of the N-domain of skeletal troponin C. Biochemistry 39:12731–12738

Millet O, Bernadó P, Garcia J, Rizo J, Pons M (2002) NMR measurement of the off rate from the first calcium-binding site of the synaptotagmin I C_2A domain. FEBS Lett 516:93–96

Millet O, Loria JP, Kroenke CD, Pons M, Palmer AG (2000) The static magnetic field dependence of chemical exchange linebroadening defines the NMR chemical shift time scale. J Am Chem Soc 122:2867–2877

Mittl PRE, Fritz G, Sargent DF, Richmond TJ, Heizmann CW, Grutter MG (2002) Metal-free MIRAS phasing: structure of apo-S100A3. Acta Cryst D 58:1255–1261

Mulder FAA, Mittermaier A, Hon B, Dahlquist FW, Kay LE (2001) Studying excited states of proteins by NMR spectroscopy. Nat Struct Biol 8:932–935

Mustafi SM, Mukherjee S, Chary KVR, Del Bianco C, Luchinat C (2004) Energetics and mechanism of Ca^{2+} displacement by lanthanides in a calcium binding protein. Biochem 43:9320–9331

Pääkkönen K, Annila A, Sorsa T, Pollesello P, Tilgmann C, Kilpeläinen I, Karisola P, Ulmanen I, Drakenberg T (1998) Solution structure and main chain dynamics of the regulatory domain (residues 1–91) of human cardiac troponin C. J Biol Chem 273:15633–15638

Pääkkönen K, Sorsa T, Drakenberg T, Pollesello P, Tilgmann C, Permi P, Heikkinen S, Kilpeläinen I, Annila A (2000) Conformations of the regulatory domain of cardiac troponin C examined by residual dipolar couplings. Eur J Biochem 267:6665–6672

Palmer AG (2004) NMR characterization of the dynamics of biomacromolecules. Chem Rev 104:3623–3640

Parker D, Dickins RS, Puschmann H, Crossland C, Howard JAK (2002) Being excited by lanthanide coordination complexes: aqua species, chirality, excited-state chemistry, and exchange dynamics. Chem Rev 102:1977–2010

Peters JA, Huskens J, Raber DJ (1996) Lanthanide induced shifts and relaxation rate enhancements. Prog NMR Spectrosc 28:283–350

Pfuhl M, Chen HA, Kristensen SM, Driscoll PC (1999) NMR exchange broadening arising from specific low affinity protein self-association: analysis of nitrogen-15 nuclear relaxation for rat CD2 domain 1. J Biomol NMR 14:307–320

Pidcock E, Moore GR (2001) Structural characteristics of protein binding sites for calcium and lanthanide ions. J Biol Inorg Chem 6:479–489

Potts BCM, Smith J, Akke M, Macke TJ, Okazaki K, Hidaka H, Case DA, Chazin WJ (1995) The structure of calcyclin reveals a novel homodimeric fold for S100 Ca^{2+}-binding proteins. Nat Struct Biol 2:790–796

Price WS (1998) Pulsed-field gradient nuclear magnetic resonance as a tool for studying translational diffusion: Part II Experimental aspects. Concepts Magn Reson 10:197–237

Prudêncio M, Rohovec J, Peters JA, Tocheva E, Boulanger MJ, Murphy MEP, Hupkes HJ, Kosters W, Impagliazzo A, Ubbink M (2004) A caged lanthanide complex as a paramagnetic shift agent for protein NMR. Chem Eur J 10:3252–3260

Rhee MJ, Sudnick DR, Arkle VK, Horrocks WD (1981) Lanthanide ion luminescence probes – characterization of metal-ion binding sites and intermetal energy-transfer distance measurements in calcium-binding proteins.1. Parvalbumin. Biochemistry 20:3328–3334

Sattler M, Schleucher J, Griesinger C (1999) Heteronuclear multidimensional NMR experiments for the structure determination of proteins in solution employing pulsed field gradients. Prog NMR Spectrosc 34:93–158

Skrynnikov NR, Dahlquist FW, Kay LE (2002) Reconstructing NMR spectra of ''invisible'' excited protein states using HSQC and HMQC experiments. J Am Chem Soc 124:12352–12360

Spyracopoulos L, Gagné SM, Li MX, Sykes BD (1998) Dynamics and thermodynamics of the regulatory domain of human cardiac troponin C in the apo- and calcium-saturated states. Biochem 37:18032–18044

Spyracopoulos L, Gagné SM, Sykes BD (2001) In: Jardetzky O, Finucane MD (eds) Dynamics, structure, and function of biological macromolecules. IOS Press, Amsterdam, pp. 37–44

Spyracopoulos L, Li MX, Sia SK, Gagné SM, Chandra M, Solaro RJ, Sykes BD (1997) Calcium-induced structural transition in the regulatory domain of human cardiac troponin C. Biochemistry 36:12138–12146

Strynadka NCJ, Cherney M, Sielecki AR, Li MX, Smillie LB, James MNG (1997) Structural details of a calcium-induced molecular switch: X-ray crystallographic analysis of the calcium-saturated N-terminal domain of troponin C at 1.75 angstrom resolution. J Mol Biol 273:238–255

Takeda S, Kobayashi T, Taniguchi H, Hayashi H, Maéda Y (1997) Structural and functional domains of the troponin complex revealed by limited digestion. Eur J Biochem 246:611–617

Takeda S, Yamashita A, Maeda K, Maéda Y (2003) Structure of the core domain of human cardiac troponin in the Ca^{2+}-saturated form. Nature 424:35–41

Tjandra N, Kuboniwa H, Ren H, Bax A (1995) Rotational dynamics of calcium-free calmodulin studied by ^{15}N NMR relaxation measurements. Eur J Biochem 230:1014–1024

Vega AJ, Fiat D (1976) Nuclear relaxation processes of paramagnetic complexes – slow motion case. Mol Phys 31:347–355

Wang CLA, Leavis PC, Horrocks WD, Gergely J (1981) Binding of lanthanide ions to troponin C. Biochemistry 20:2439–2444

Weis WI, Kahn R, Fourme R, Drickamer K, Hendrickson WA (1991) Structure of the calcium-dependent lectin domain from a rat mannose-binding protein determined by MAD phasing. Science 254:1608–1615

Yap KL, Ames JB, Swindells MB, Ikura M (1999) Diversity of conformational states and changes within the EF-hand protein superfamily. Proteins 37:499–507